Designing Polylactide/Clay Nanocomposites for Textile Applications: Effect of Processing Conditions, Spinning, and Characterization

Samuel Solarski,[1] Manuela Ferreira,[1] Eric Devaux,[1] Gaëlle Fontaine,[2] Pierre Bachelet,[2] Serge Bourbigot,[2] René Delobel,[2] Philippe Coszach,[3] Marius Murariu,[4] Amália Da Silva Ferreira,[4] Michael Alexandre,[4] Philippe Degee,[4] Philippe Dubois[4]

[1]Ecole Nationale Supérieure des Arts et Industries Textiles (ENSAIT), Laboratoire de Génie et Matériaux Textiles (GEMTEX), UPRES EA2461, 9 rue de l'Ermitage, BP 30329, 59056 Roubaix Cedex 01, France
[2]ENSCL Laboratoire PERF, LSPES UMR/CNRS 8008, Avenue Dimitri Mendeleïev Bât. C7a, BP 108–59652 Villeneuve d'Ascq Cedex, France
[3]Galactic s.a., Place d'Escanaffles, 23 BE 7760 Escanaffles, Belgique
[4]Service des Matériaux Polymères et Composites, Université de Mons-Hainaut and Materia Nova, Place du Parc 20, B-7000 Mons, Belgique

ABSTRACT: An experimental study was carried out to design polylactide (PLA)-clay nanocomposites for developing fibers. PLA and 1–10 wt % of a selected organomodified bentonite (Bentone® 104-B104) were melt mixed to examine the effect of processing conditions (temperature, shear, residence time) on the morphology of performed polymer nanocomposites (PNC). Because of a good compatibility with PLA matrix, the dispersion of B104 occurred under different conditions without difficulty, and a similar morphology was obtained. The results obtained showed that at low temperature of mixing, the shear stress exerted on polymer has a key role on the extent of intercalation and delamination. Upscale experiments were further performed using optimized conditions and 4 wt % B104 was added to PLA matrix by melt blending to produce PNC for spinning. Then, the recovered PNC were melt spun to produce multifilaments yarns, and it was demonstrated that surprisingly, it is not necessary to use a plasticizer to spin a blend with 4 wt % B104. The properties of the yarns have been studied in terms of clay dispersion as well as thermal, mechanical, and shrinkage properties. B104 could be added up to 4 wt % into PLA without detrimentally sacrificing the tensile strength of melt-spun filaments, especially at high draw ratio. Interestingly, the PNC-based multifilaments were knitted and the flammability studied using cone calorimeter at 35 kW/m². A strong decrease, up to 46%, of the heat release rate was measured. © 2008 Wiley Periodicals, Inc. J Appl Polym Sci 109: 841–851, 2008

Key words: polylactide; nanocomposites; processing; melt spinning

INTRODUCTION

Biodegradable polymers have found confirmation in textile applications and polylactide (PLA) seems to be one of the most promising candidates for future developments; it is not only biodegradable but also produced from renewable resources. Because PLA has been recently considered as alternative in replacing petrochemical polymers, there is a strong demand to enlarge its properties, first by combining this matrix with different dispersed phases: nanofillers, additives, plasticizers, other polymers, etc.

Nanofillers, as clay and more particularly montmorillonite, are well known to modify the properties of polymers when they are blended even at low filler level (generally under 5% in weight).[1,2] Generally, thermal, mechanical, flammability, and barrier properties can be strongly improved. The polymer nanocomposites (PNC) are interesting to develop nanocomposites-based fibers with new properties. The use of a polymeric matrix to produce a nanocomposite multifilament yarn has been described for the first time in 2002 by Bourbigot et al.[3] The matrix used was polyamide 6 (PA6) reinforced with Cloisite®30B (C30B). The flammability of knitted structure made with PA6 and PA6/C30B was investigated, and a strong decrease of the heat release rate was measured. Then, some nanocomposite matrices were used to develop some new kind of fibers: polyamide (PA),[4] polybutylene terephthalate (PBT),[5]

polytrimethylene terephthalate (PTMT),[6] polyethylene terephthalate (PET),[7–9] polypropylene (PP),[10,11] and polyimideamide (PIA).[12,13] Until now, only few polymer/clay blends have been studied for the production of fibers. When clay is added, the thermal, fire, and dimensional stability properties of filaments are generally improved. As far as the mechanical properties are concerned, some authors have observed an improvement, particularly when nanocomposite filaments are not drawn. The drawing stage of nanocomposites filaments leads to a decrease of the mechanical properties. Yoon et al.[4] measured an increase of the Young's modulus of PA with a 5 wt % filler, but tensile strength and elongation at break decreased. Chang et al. have shown that the tensile strength and the Young's modulus of PTMT[6] and PET[7] nanocomposite filaments not drawn increased with the clay level. On the other hand, if the filaments are drawn, the tensile strength decreases. Mikołajczyk et al.[13] also observed that PIA nanocomposite fibers have lower strength properties when compared with those ones without montmorillonite.

On the other hand, in the melt-processing route of PLA-clay compositions, the rheological and thermodynamic characters of the materials are important parameters that can determine the degree of intercalation/exfoliation and properties of the final polymer nanocomposites. Recent studies realized by using different polymers (e.g., polyamides and polypropylene) have demonstrated that melt-processing conditions play a key role in achieving high levels of intercalation and/or exfoliation. The degree of clay dispersion in the mixing process is governed by the matrix viscosity, average shear rate, and the mean residence time. In addition, proper choice of clay and surface organomodification is also critical.[14,15]

Obviously, for some polymer-organoclay systems, the quality of a potential PNC is imposed by a huge number of restrictions such as the processing conditions and/or type of equipment available to perform these PNC. On the other hand, from the perspective of application, it is believed that this advanced dependence between the fabrication process and nanocomposites morphology may lead to important variations concerning the quality of final products, for example, fibers. Thus, technologically speaking, a higher "flexibility" during preparation of PNC is imperiously required.

In a previous work, we have studied the possibility to develop polylactide/clay nanocomposite filaments.[16] We have shown that problems to spin occurred for PLA filled with more than 2 wt % of C30B. The elongation at break strongly decreases, and so filaments with low tensile properties were obtained. For this reason, a blend with dioctyl adipate as plasticizer (10 wt %) was prepared and the resulting sample was extruded and successfully melt-spun drawn. The filaments obtained have better elongation properties, so that they could be used to produce knitted fabrics. It was shown that only 2 wt % of C30B was enough to improve the fire behavior of the knit.

In this context, from the multitude of organoclays that can be blended with PLA matrix, after a preliminary selection (not discussed here) a bentonite modified with benzyl dimethyl hydrogenated tallow ammonium has been considered as attractive for preparation of PNC designed for the fabrication of fibers.

The first objective of this article is to show how much the dispersion of Bentone 104 (Elementis Specialties) into PLA matrix is sensitive to the processing conditions. Therefore, in a first experimental step, combinations of up to 10 wt % organoclay and high molecular weight PLA were carried out at laboratory scale by using a microcompounder in corotating mode and deeply characterized. The second objective is to discuss about the potentiality of Bentone 104 to develop PLA/clay nanocomposite filaments without any plasticizer.

EXPERIMENTAL

Materials

An organomodified layer silicate supplied as Bentone 104 (B104, supplier-"Elementis Specialties") in which the exchange cation is benzyl dimethyl hydrogenated tallow ammonium (131 mequiv/100 × g clay, ∼ 70 wt % content in inorganic) was used for melt-blending experiments after a previous drying during 60 min at 130°C under vacuum.

Poly(L,L-lactide) (PLA) sample-commercial name "GALASTIC," was supplied by Galactic S.A. and used as biodegradable polyester matrix (characteristics of this PLA are as follows: M_n (PLA): 74,500 g/mol, L/D-isomer ratio of ∼ 96 : 4, residual monomer: 0.18 wt %, relative viscosity: 3.96). Before processing by melt compounding or by melt -spinning, PLA was dried under vacuum 12 h at 80°C.

Sample preparation

Nanocomposite preparation by melt-compounding

PLA-Galastic® is a grade designed for extrusion due to a reduced fluidity in the molten state (high molecular weights). Both polyester matrix and organoclay were intensively dried under vacuum (see Materials and methods section) to limit partial PLA degradation induced by water at the processing temperature. The melt compounding of the PLA-clay blends was performed under selected conditions according to experimental procedure shown in Figure 1 (temperature: 180–220°C, speed of the screws from 50–250
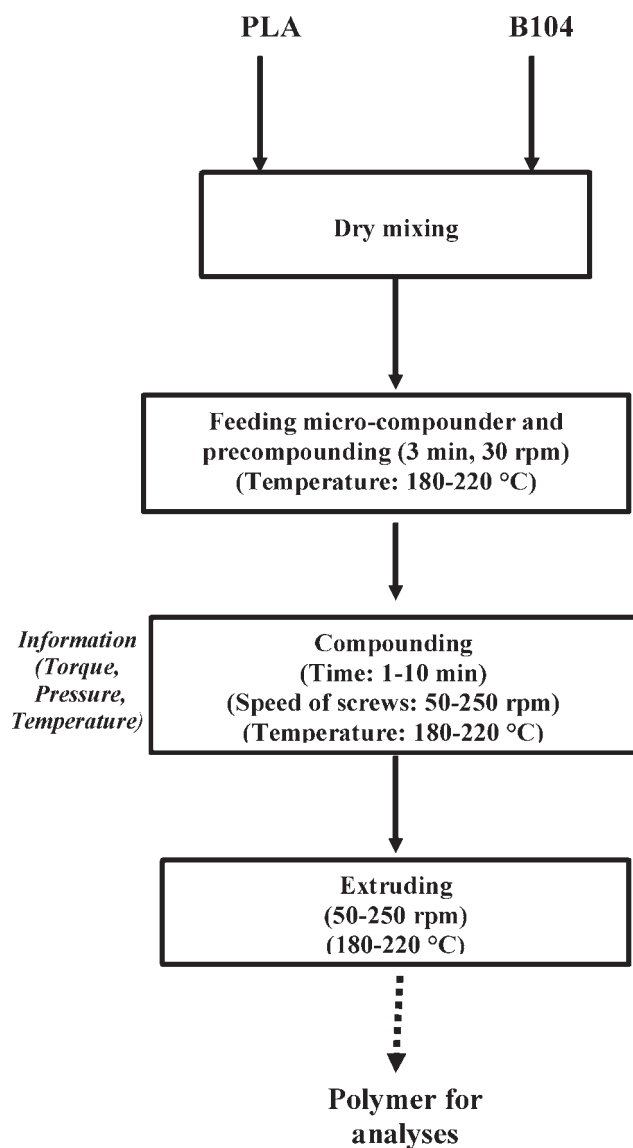
PLA   **B104**

Figure 1 Schematic illustration of the experimental procedure for realization of PLA-nanocomposites using the Thermo Haake microcompounder.

rpm, estimated residence time from 1–10 min). For nanocomposites preparation, combinations from 1–10 wt % clay (content in inorganic) and PLA were first dry-mixed by shaking them in glass ampoules. Then, the melt compounding of PLA-clay blends was performed under different processing conditions by using the MiniLab Rheomex CTW5 (Thermo Haake), a conical intermeshing twin-screw microcompounder (corotating mode, coefficient of filling of ~ 0.7).

At upscale, PLA nanocomposite used to be melt spun are prepared through melt-direct intercalation by using a conventional polymer extrusion process and optimized parameters. PLA pellets with 4 wt % B104 are blended using a corotating twin-screws extruder (Thermo Haake, diameter of screw (D) =

16 mm, $L/D = 25$). The temperatures of the five zones are 140, 160, 170, 180, and 190°C. The rotation speed is maintained at 150 rpm. PLA and B104 are incorporated together in a first feeding zone. The extrudate is then pelletized.

Melt spinning

PLA and PLA nanocomposites are spin drawn with the spinning device Spinboy I from Busschaert Engineering. PLA multifilament yarns with 4 wt % B104 are obtained. Pellets are first melted in a single screw extruder from 210–215°C. Then melted PLA passes through two dies consisting of 40 channels with a diameter of 400 μm to obtain a multifilament continuous yarn, which is coated with Filapan CTC (blend of branched acid ester and branched polyglycol), a spin finish supplied by Boehme. At last, the multifilament yarn is hot drawn between two rolls: the draw ratio (DR), which is the ratio between the rotation speeds of the feeding and the draw rolls (first and second rolls, respectively), varies from 2–3.5. The speed of the feeding roll is maintained at 200 m/min, and the speed of the draw roll varies from 400–750 m/min. The temperature of the first roll is 70°C, and the temperature of the second roll is 110°C.[17]

Knitting

Multifilament yarns made with PLA, PLA/4 wt-% B104 are knitted manually on a rectilinear machine gauge 8. The multifilaments used have undergone the highest draw ratio (3.5 for PLA and PLA/4 wt % B104). These multifilaments have a fineness of ~ 1600 dtex (dtex = 10^{-1} g/1000 m). Knitted fabrics with a surface weight of 1000 g/m^2 and a thickness of 3 mm are obtained.

Characterization methods

Investigation of the dispersion of B104

The dispersion of clay in PLA/B104 pellets and PLA/4 wt % B104 filaments is analyzed using wide-angle X-ray diffraction (WAXD) and transmission electron microscopy (TEM).
WAXD. The morphological analysis by X-ray diffraction was performed on a Siemens D5000 diffractometer using Cu Kα radiation (wavelength: 1.5406 Å) at room temperature in the range of 2θ = 1.5–30°, by step of 0.04° and scanning rate of 2°/min.
TEM. Transmission electron micrographs were obtained with a Philips CM100 apparatus using an accelerator voltage of 100 kV. The samples were 70–80-nm thick and prepared with a Reichert Jung Ultracut 3E, FC4E ultracryomicrotome cutting at −130°C. Reported microphotographs represent typi-

cal morphologies as observed at, at least, three various places of, at least, three different slices.

Characterization of thermal stability of PLA pellets

Thermogravimetry analyses (TGA) of PLA nanocomposites were performed by using a TGA Q50 from TA Instruments with a heating ramp of 20°C/min under atmospheric air flow (platinum pans, 60 cm³/min air flow rate).

Characterization of thermal properties of PLA pellets and fibers

The thermal characteristics of PLA and fibers are investigated using a TA Instruments DSC 2920 with the modulation option. To separate the glass transition and the relaxation phenomenon, the underlying rate used is 1°C/min, with amplitude of 1°C and a period of 60 s. These parameters allow observing the glass transition in the reversing curve and the relaxation phenomenon in the nonreversing one. To observe the cold crystallization and the melting, the underlying rate used is 5°C/min with amplitude of 0.769°C and a period of 60 s. All experiments are carried out using helium as purge gas.

Characterization of the tensile properties of PLA fibers

The measurement of the tensile properties of PLA and PLA/4 wt % B104 filaments have been carried out following the standard NF EN ISO 5079 on a tensile testing machine Zwick 1456, the cell force used is 10N. All the tests have been made at standard atmosphere (the temperature is 20°C ± 2°C and the relative humidity is 65% ± 5%). The length between the clamps is 20 mm. All the results represent an average value of 50 tests.

Shrinkage of multifilaments yarn

The shrinkage of PLA and PLA/4 wt % B104 multifilaments has been measured at 80°C. The multifilaments (with an initial length L_0 of 1 m) are heated in hot air for 10 min without pretension. Then the multifilaments are maintained at the ambient air during 20 min. Then a pretension of 0.4 cN/tex is applied during 30 s, and the final length (L_f) of the multifilaments is measured. The shrinkage (S) is given by the following equation:

$$S = \frac{L_0 - L_f}{L_0} \times 100$$

Cone calorimetry by oxygen consumption

Knitted fabrics (100 × 100 × 3 mm³) were exposed in horizontal orientation in a FTT Cone Calorimeter,

to an external heat flux of 35 kW/m². This heat flux has been chosen, because it represents common heat flux in mild fire scenario.[18,19] All the experiments were repeated thrice to check the reproducibility. The cone calorimeter was used to determine some fire properties, and particularly the rate of heat released (RHR) and the total heat evolved (THE), which is the cumulated heat released, and time to ignition (t_{ig}).

RESULTS AND DISCUSSION

In a first experimental step, PLA-based nanocomposites with different compositions were obtained under different conditions using the Thermo Haake microcompounder to study the effect of processing parameters on morphology and thermal properties of the nanocomposites prepared. The extent of intercalation or exfoliation was studied through WAXD and TEM analyses, whereas the modifications concerning the thermal stability were evaluated by TGA analysis.

Effects of processing parameters and composition on morphology and thermal properties

Temperature dependence

Figure 2(A) shows WAXD patterns of B104 and of PLA/3 wt % B104 nanocomposites prepared at different temperatures, that is, 180, 200, and 220°C (residence time: 5 min; shear rate: 150 rpm). As far as the quality of B104 dispersion is considered, the results obtained show that the temperature of processing is a key parameter that must be considered to control the quality of clay dispersion. PLA nanocomposites prepared at 180°C are displaying a broadening of the diffraction peak of B104 (initial peak 2θ angle of 4.4°, $d_{001} \sim 2.00$ nm) to lower 2θ angle suggesting that the clay is less ordered and likely well dispersed. For other melt-blending conditions, for example, at lower viscosity (temperature of 220°C), presence of predominately intercalated clay layers is more easily detected from WAXD patterns as attested for by the presence of an important sharp peak at $\sim$ 2θ angle of 2.5° ($d_{001} \sim 3.53$ nm).

TEM images (Fig. 3) confirm the results from WAXD analyses attesting for a good quality of dispersion of B104 in PLA. Anyway, it is difficult to perform the exact quantification of the intercalation/exfoliation process even when comparing extreme melt-compounding temperatures, that is, 180 and 220°C. Nevertheless, at lower mixing temperature [180°C; Fig. 3(A,B)], the orientation of sheet nanostructures in the direction of extrusion seems to be more pronounced. At low magnification, the images show a homogeneous dispersion of the primary clay
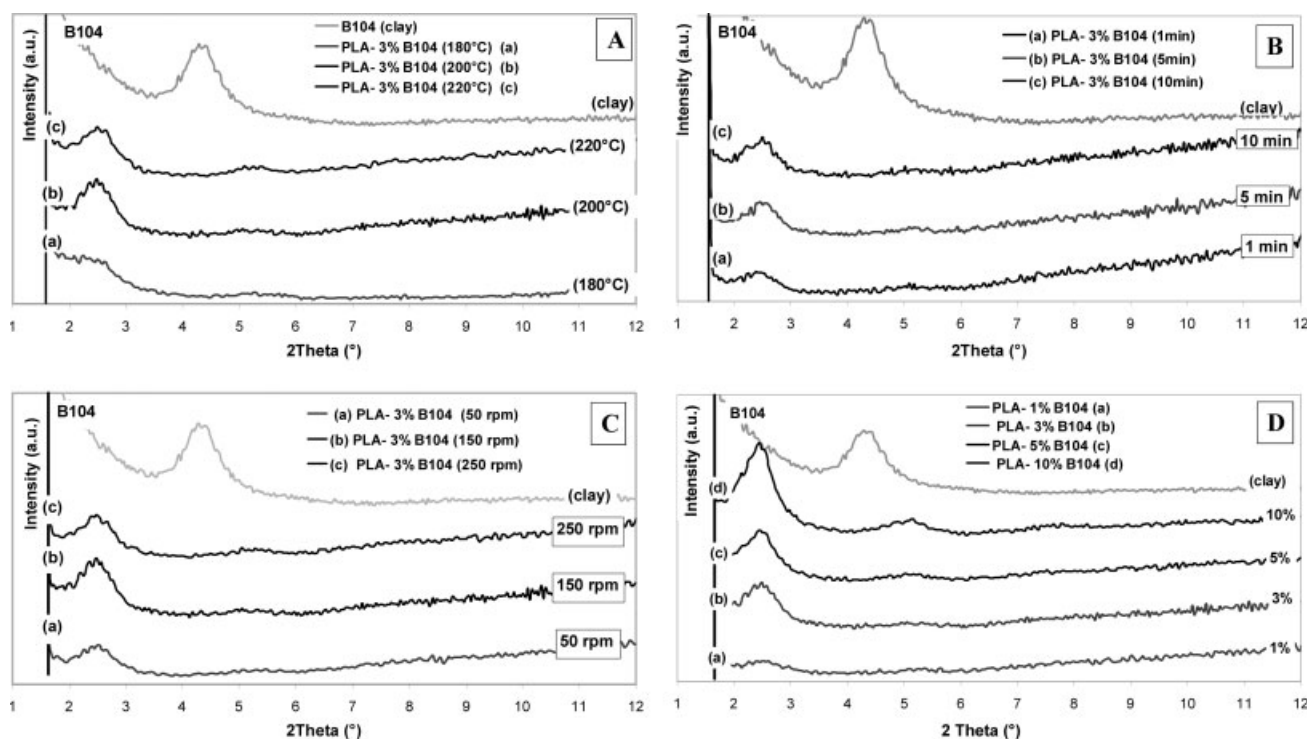
Figure 2 WAXD patterns of PLA/B104 nanocomposites showing the effect of processing parameters and clay percentage: A-temperature: blends performed at 180–220°C (150 rpm, 5 min); B-residence time: 1–10 min (200°C, 150 rpm); C-shear conditions: 50–250 rpm (200°C, 5 min); D-clay percentage: 1–10 wt % (200°C, 150 rpm, 5 min).

particles throughout the PLA matrix. At higher magnification, a mixed morphology is evidenced, which contains large amount of exfoliated silicate sheet nanostructures resulting from an extensive penetration of PLA matrix between the organoclay layers and some intercalated nanostructures that are homogeneously dispersed into polymer matrix. On the other hand, at lower melt viscosity, as obtained by increasing the temperature of melt-compounding to 220°C, TEM images [Fig. 3(C,D)] suggest a decrease in the quality of the orientation of the sheet nanostructures with the direction of extrusion. The size of the stacks seems also a bit larger, especially on the high magnification image [Fig. 3(D)], when compared with the sample prepared at 180°C [Fig. 3(B)]. Accordingly, a better morphology (intercalated/ delaminated) seems to be obtained where the viscosity of the system is high enough (e.g., at 180°C) due to a higher level of the shear stress transferred between the polymer matrix and clay.

Otherwise, because the clay particles can be more oriented, the reduction of processing temperature does not lead to any worsening effect on the final morphology, therefore, temperatures of 180–200°C can be considered as optimal for further/upscale experiments to produce PLA nanocomposites designed for the realization of fibers.

Concerning the thermal behavior, all studied samples are characterized by similar thermal stability, without any significant differences in the TGA thermograms (temperature at 5% weight loss = 352°C ± 3°C and temperature for the maximum rate of degradation = 397°C ± 5°C whatever the processing temperature).

Time of mixing

The time of mixing is usually considered as "critical parameter" for diverse polymer-organoclay systems that are obtained by melt blending. Surprisingly, in the presence of B104, results from WAXD analyses [Fig. 2(B)] show that the prepared PNC are characterized by a similar level of intercalation whatever the investigated residence time, actually ranging from 1 to 10 min. Indeed, the $d_{(001)}$ peak does not change appreciably in position and size with residence time at constant shear stress (200°C and 150 rpm). This demonstrates that for PLA-B104 system the thermodynamically stable state is reached in relatively short time.

On the other hand, generally, it is believed that by increasing the residence time, as already reported for some PA-clay systems,[20] an improved level of delamination and dispersion can be expected. However, besides the level of intercalation, the residence time may play a role on the amount of sheets in the intercalated stacks. Indeed, in our case, longer residence time may lead to a reduction of the mean
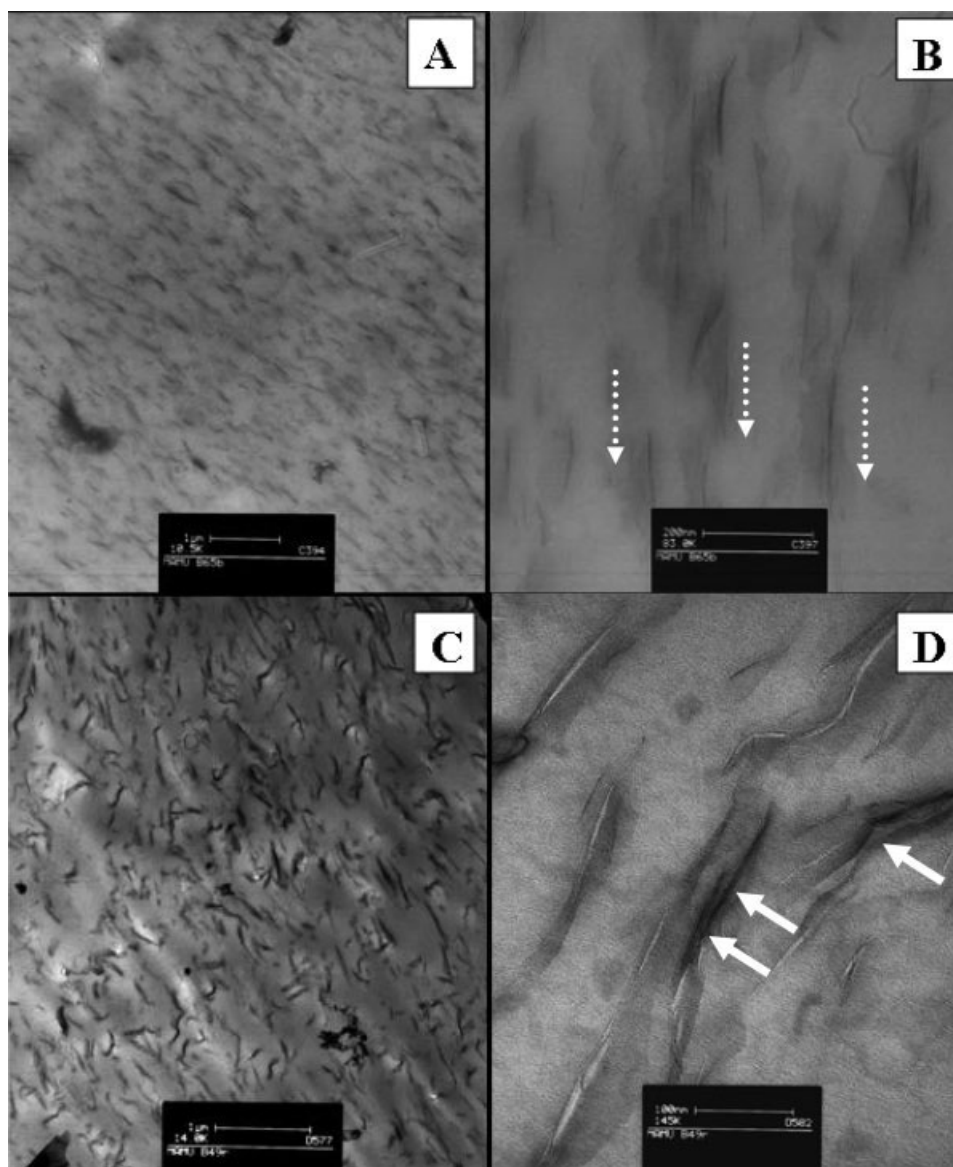
Figure 3 TEM pictures of PLA/3 wt % B104 nanocomposites performed by using high shear conditions (150 rpm, 5 min) at different temperatures: 180°C (low magnification (scale of 1 μm)-A and high magnification (200 nm)-B) and 220°C (low (1 μm)-C and high magnification (100 nm)-D).

number of sheets by stacks and therefore a better overall dispersion of clay within the material.

TG analysis [Fig. 4(A)-PLA-3 wt % B104 for 1- and 10-min residence time] does not reveal any significant differences that could be correlated to the mixing time, thus it could be concluded that by using the established experimental procedure; B104 is readily dispersed, even within a short residence time. On the contrary, it is however expected that some negative effects could be recorded at higher temperature of mixing (e.g., at 220°C) and longer residence time due to the relatively low thermal stability of the organomodifier and the known sensitivity of PLA to transesterification reactions under shear conditions.

Shear dependence

Experiments carried out under various shear conditions (rotation speed from 50–250 rpm for a common residence time of 5 min at 200°C) show that B104 can be intercalated/delaminated and dispersed into PLA matrix without any difficulty.

WAXD analyses of PLA/3 wt % B104 compositions do not reveal any significant differences on the extent of clay intercalation [Fig. 2(C)], and the effect of shear is not that much evident. Moreover, as results from TGA, these samples are characterized by similar thermal behavior without any marked shift of the onset temperature of degradation or of the temperature of maximal weight loss rate (tem-
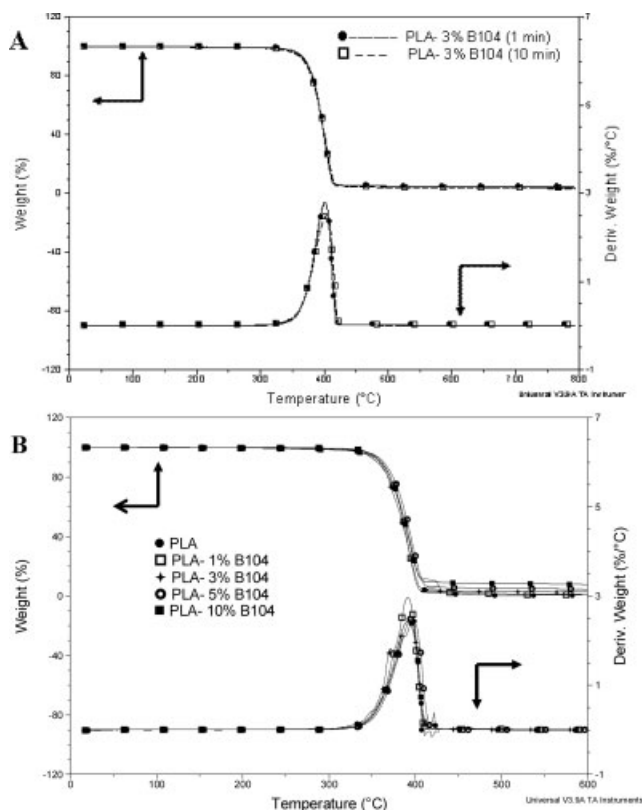
Figure 4 TGA and d-TGA traces of PLA/B104 nanocomposites (ramp of 20°C/min under air flow) showing the effect of residence time and clay percentage: A-residence time: 1 and 10 min (200°C, 150 rpm); B-clay percentage: 0–10 wt % (200°C, 150 rpm, 5 min).

perature at 5% weight loss = 351°C ± 2°C and temperature for the maximum rate of degradation = 396°C ± 4°C whatever the shear during melt compounding).

Clay relative content

Figure 2(D) shows WAXD patterns of PLA and PLA/1–10 wt % B104 nanocomposites prepared at 200°C for 5 min residence time by using high shear conditions (150 rpm).

As it was expected, the increase of clay percentage leads to some differences between the morphology of the performed nanocomposites that are the most probably in correlation with the quality of the dispersion/exfoliation. Indeed, Tanoue et al.[21] have calculated that for nanocomposites based on clay sheets with aspect ratio around 100–500, the clay nanosheets should begin to geometrically interact with each other for content higher than 1.2 wt %.

This is a confirmation for the hypothesis that at higher clay levels, equilibrium between exfoliation and intercalation is drawn toward intercalation. A predominately intercalated morphology seems to be typically observed for the highly filled samples (e.g.,

10 wt % B104), whereas for lower percentage of clay, for example, 3 wt %, the exfoliation/intercalation of the clay layers is reached as already established by TEM analyses.

Concerning the thermal stability, conventional TGA performed under air on the resulting PLA nanocomposites and pristine PLA realized in the conditions of this experimental procedure does not show any significant effect of the clay content on the temperature for the maximum rate of thermal degradation of the PLA matrix [Fig. 4(B)].

Finally, for all PLA-B104 nanocomposites, an increase by 7–12°C of the temperature at 5% weight loss can be noticed when comparing with the pristine PLA (temperature at 5% weight loss = 343 ± 4°C). Such an increase can be associated to the presence of the nanodispersed clay phase.

Study of the properties of PLA nanocomposites filaments

Dispersion of clay in PLA/4 wt % B104 filaments

Figure 5 represents the WAXD curves of B104, PLA/4 wt % B104 (pellets and filaments with a draw ratio of 3.5). The characteristic peak of B104, located at 4.4°, is shifted toward lower angle (2.5°) when B104 is blended with PLA. The decrease of the diffraction angle means that PLA macromolecules crawl in and insert between the silicate layers of B104. By using the Bragg's law, it is possible to calculate the d_{001} value, which is the interlayer space. For B104 and PLA/B104 pellets, d is respectively, 2.00 and 3.53 nm. It represents an increase of the interlayer space, d_{001}, of 1.53 nm. So, a nanocomposite with a predominately intercalated structure is obtained. On the other hand, as far as the PLA/4 wt % B104 filaments are concerned, no peak is observed in the low angle area. The disappearance of the characteristic peak suggests that the nanocomposite structure of the filaments is rather exfoliated or disordered.

The nanocomposite structure of the PLA/4 wt % B104 filaments has also been observed using TEM [Fig. 6(A,B)]. The image at low magnification shows a dispersion of the silicate layers rather homogene-
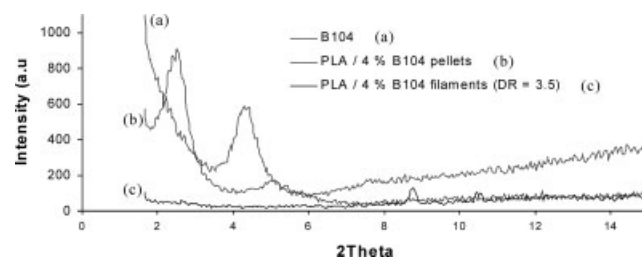

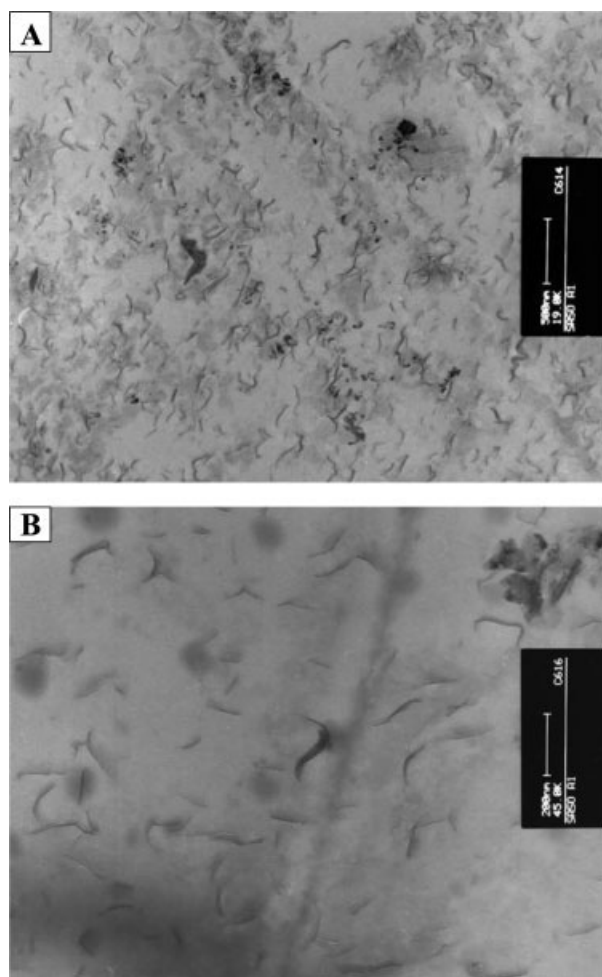**Figure 5** XRD curves of B104, PLA/4 wt % B104 (pellets and filaments).

Figure 6 TEM images of PLA/4 wt % B104 filaments. (A) and (B) represent respectively, the cross sections at low (500 nm) and high (200 nm) magnification.

ous, even if some little tactoids are still present. A lot of exfoliated layers can be observed in Figure 6(B). Drawing seems to have a strong effect on the nanocomposite structure. From an intercalated structure for PLA/4 wt % B104 pellets, it turns to get exfoliated when PLA/4 wt % B104 is melt spun and drawn. The shear induces during the drawing would make the separation of silicate layers easier in the filaments. The TEM images, which represent the cross sections of the filaments, show rather well-defined dark lines (i.e., borders of the silicate layers). An orientation of the silicate layers in the drawing direction can be assumed. This effect was already observed after the extrusion of PLA and B104 (see temperature dependence section).

Mechanical properties

Figure 7 represents the Young's modulus values of the PLA and PLA/4 wt % B104 filaments. Compared with unfilled PLA, the Young's modulus values of
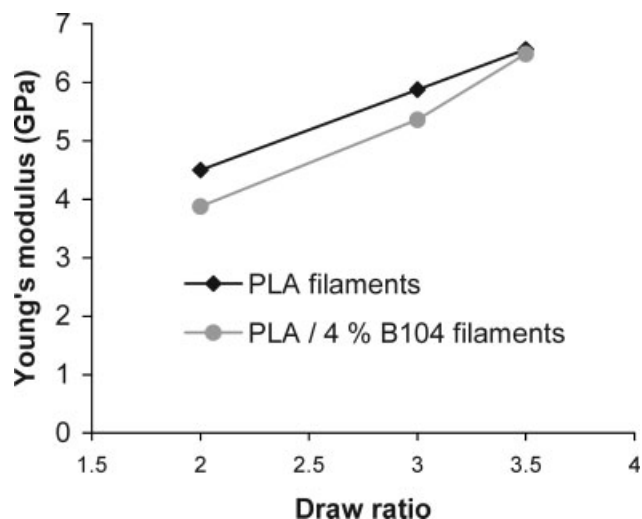
Figure 7 Young's modulus of PLA and PLA/4 wt % B104 filaments.

PLA/4 wt % B104 filaments are slightly lower when the draw ratio is lower or equal to three. For the highest studied draw ratio, there is no difference recorded. In this case, the value of the Young's modulus is 6.5 GPa. It is a strong advantage compared with C30B, which leads to a decrease of the Young's modulus. The values of the tensile strength for PLA and PLA/4 wt % B104 are presented in Figure 8. The presence of 4 wt % B104 leads to a decrease of the tensile strength whatever the draw ratio applied. For the highest studied draw ratio, the tensile strength of PLA and PLA/4 wt % B104 filaments is 415 and 353 MPa, respectively, which represents a decrease by 15%.

It is interesting to notice that drawing seems to reduce the difference between the values of tensile
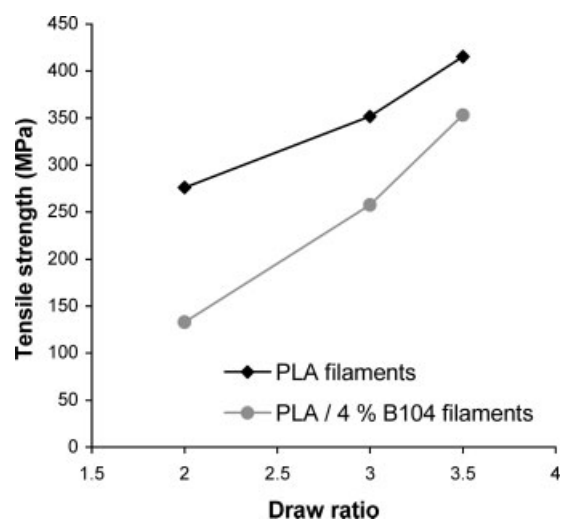

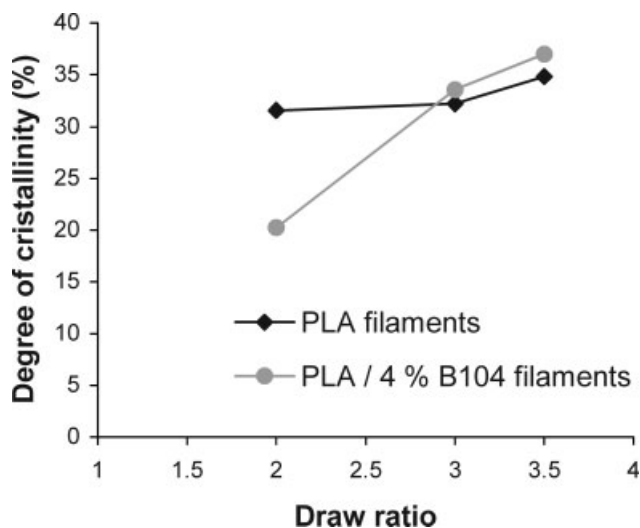**Figure 8** Tensile strength of PLA and PLA/4 wt % B104 filaments.

Figure 9 Degree of crystallinity of PLA and PLA/4 wt % B104 filaments.

Thermal properties

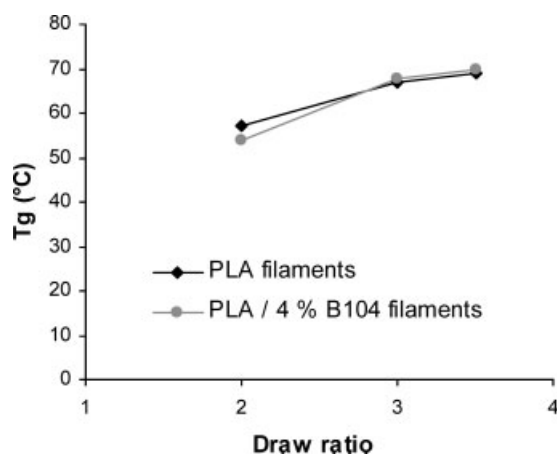Figure 9 represents the degree of crystallinity of PLA and PLA/4 wt % B104 filaments as a function of the draw ratio. At low draw ratio (DR = 2), the degree of crystallinity of PLA/4 wt % B104 is lower with regards to unfilled PLA filaments. The same effect was observed with PLA filaments filled with C30B.[16] For the highest studied draw ratio, the values of degree of crystallinity are similar. One can suppose that for PLA nanocomposite drawn at low draw ratio, the silicate layers limit the crystallization. As for the PLA filaments, the glass transition temperature of PLA/4 wt % B104 increases with the draw ratio (cf. Fig. 10), the presence of silicate layers does not modify the values of T_g. For a low draw ratio (DR = 2), the T_g is 54.3°C for PLA/4 wt % B104 filaments and increases up to 69.5°C when DR = 3.5. So, the thermal properties of PLA nanocomposite filaments are very similar to the values recorded for the unfilled filaments.

strength of PLA and PLA/4 wt % B104 filaments. For a low draw ratio (DR = 2), the difference is 51.8%. For an intermediate draw ratio (DR = 3), it is 26.8% and only 15.0% for the highest draw ratio (DR = 3.5). This decrease of the difference with the increase of the draw ratio can be explained by a preferential orientation of the silicate layers during drawing. At low draw ratio, the silicate layers in the filaments are not oriented in the drawing direction, contrary to those present in filaments drawn at maximal draw ratio. When considering the elongation at break, no difference is measured between unfilled PLA and PLA/4 wt % B104 filaments.

Shrinkage properties of PLA nanocomposite filaments

The shrinkage values of PLA and PLA/4 wt % B104 filaments are presented in Figure 11. Interestingly, whatever the temperature of the test and the DR applied on the filaments, the shrinkages values for the PLA/4 wt % B104 remain lower in regards with the values of unfilled PLA filaments. This phenomenon has already been observed with some PLA[16] and PET[9] fibers modified with nanofillers. The silicate layers of B104 can decrease the molecular mobility of the macromolecules inserted between the silicate layers or in their vicinity. So, these macromolecules are less sensitive to heat and need higher temperature to shrink.

Figure 10 Glass transition temperature of PLA and PLA/4 wt % B104 filaments.

Reaction to fire of PLA nanocomposite filaments

The cone calorimeter is an efficient equipment to study the reaction to fire of a material. It allows to determine a large number of parameters, which can describe the fire behavior of a material as the time to ignition (t_{ig}), the rate at which the heat is released (RHR), the total heat that is released (THR), the volume and toxicity of smoke produced. Two kinds of
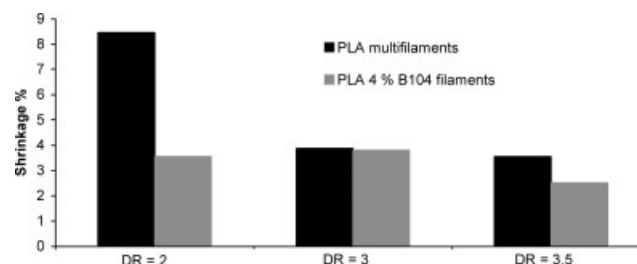

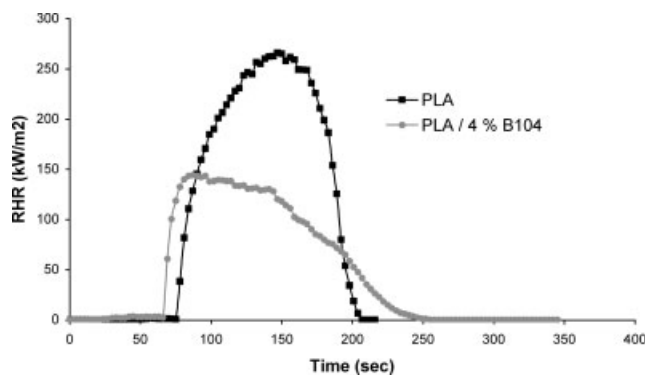**Figure 11** Shrinkage properties of PLA and PLA/4 wt % B104.

Figure 12 RHR curves of PLA and PLA/4 wt % B104-knitted fabrics.

samples (PLA and PLA/4 wt % B104 filaments) have been knitted to study the influence of the B104 content on reaction to fire.

Figure 12 represents the RHR curves of PLA and PLA/4 wt % B104 knitted fabrics. The time to ignition of PLA knitted fabric occurs at 76 s. When PLA is filled with B104, t_{ig} is only 66 s. The decrease of t_{ig} of a polymer matrix filled with clay has already been observed.[3,22] This decrease can be assigned to the difference of thermal conductivity between PLA and PLA nanocomposite knitted fabrics. The presence of clay decreases the thermal conductivity of PLA nanocomposite compared with neat PLA. The consequence is a higher accumulation of heat at the surface of PLA nanocomposite-knitted fabrics. So for, PLA nanocomposite, the ignition temperature is reached quicker than for neat PLA. It can also be assigned to the fibrillation of the multifilament yarn. Short fibers are visible at the surface of the knitted fabrics. They can act as small matches leading to the shortening of the ignition time. For PLA-knitted fabric, the maximal value for RHR is 265 kW/m². In case of PLA/4 wt % B104 knitted fabrics, the maximal value is 143 kW/m², which represents a decrease of 46%. The decrease of RHR peak value can be explained by the formation of a char, which is clearly seen when nanocomposites-based knitted fabrics are burning. This char has a double effect. It can prevent the small flammable molecules formed during degradation from being released and prevent or at least refrain the oxygen molecules to diffuse into the material. The char can also protect the material from the heat by forming an insulating barrier.

CONCLUSIONS

Blends of PLA and a selected organomodified bentonite were melt mixed in a microcompounder to examine the effect of processing conditions on the morphology and thermal properties of the performed nanocomposites. The influence of different parameters such as temperature, shear, residence time as well as the organoclay content was evaluated by traditional techniques. WAXD and TEM results revealed a mixed structure of PLA-based nanocomposites, having regions of intercalated and exfoliated clay platelets. Because of a good compatibility with PLA matrix, the dispersion of B104 occurs under different processing conditions without any difficulty. Results obtained for different mixing times showed that at constant high shear stress intercalation of clay sheets can be obtained in a short residence time. The best results in the perspective of upscale experiments demonstrated that the shear stress transferred between polymer and clay at lower temperature of mixing has a key role on the extent of intercalation and delamination.

Upscale experiments have been realized and PLA nanocomposite filaments were obtained by using B104 as filler. The study of morphology using WAXD and TEM shows an excellent dispersion of this clay into the PLA filaments. The thermal properties measured using MDSC are not strongly modified. As far as the mechanical properties are concerned, they are somehow lower when B104 is added to PLA. But this difference decreases when the draw ratio increases, especially for the tensile strength. This phenomenon could be explained by the orientation of the silicate layers during the drawing process. B104 seems to be more suitable to develop polymer-layered silicate nanocomposite filaments. In contrast to previously investigated C30B, this clay can be added up to 4 wt % without detrimentally affecting the tensile strength properties of melt-spun filaments, especially when filaments are drawn at high draw ratio. Moreover, it is not necessary to use a plasticizer, which undoubtedly simplifies the extrusion process of PLA and B104.

The incorporation of 4 wt % B104 improves the shrinkage properties and reaction to fire of filaments. Such an effect is of key interest because this the ''nano effect'' can be considered as permanent (i.e., the separated nanoplatelets are imbedded within the matrix), contrary to some classical textile finishes, which are sensitive to washes.

References

1. Alexandre, M.; Dubois, P. Mater Sci Eng 2000, 28, 1.
2. Ray, S. S.; Okamoto, M. Prog Polym Sci 2003, 28, 1539.
3. Bourbigot, S.; Devaux, E.; Flambard, X. Polym Degrad Stab 2002, 75, 397.
4. Yoon, K.; Polk, M. B.; Min, B. G.; Schiraldi, D. A. Polym Int 2004, 53, 2072.
5. Chang, J. H.; An, Y. U.; Kim, S. J.; Im, S. Polymer 2003, 44, 5655.
6. Chang, J. H.; Kim, S. J.; Im, S. Polymer 2004, 45, 5171.
7. Chang, J. H.; Kim, S. J.; Joo, Y. L.; Im, S. Polymer 2004, 45, 919.
8. Chang, J. H.; Kim, S. J. Polym Bull 2004, 52, 289.

9. Xiao, W.; Yu, H.; Han, K.; Yu, M. J Appl Polym Sci 2005, 96, 2247.
10. Pavliková, S.; Thomann, R.; Reichert, P.; Mülhaupt, R.; Marcinćin, A.; Borsig, E. J Appl Polym Sci 2003, 89, 604.
11. Zhang, X.; Yang, M.; Zhao, Y.; Zhang, S.; Dong, X.; Liu, X.; Wang, D.; Xu, D. J Appl Polym Sci 2004, 92, 552.
12. Mikołajczyk, T.; Olejnik, M. J Appl Polym Sci 2006, 101, 1103.
13. Mikołajczyk, T.; Rabiej, S.; Olejnik, M.; Urbaniak-Domagała, W. J Appl Polym Sci 2007, 104, 339.
14. Fornes, T. D.; Yoon, P. J.; Keskkula, H.; Paul, D. R. Polymer 2001, 42, 9929.
15. Yang, K.; Ozisik, R. Polymer 2006, 47, 2849.
16. Solarski, S.; Mahjoubi, F.; Ferreira, M.; Devaux, E.; Bachelet, P.; Bourbigot, S.; Delobel, R.; Coszach, P.; Murariu, M.; Da Silva Ferreira, A.; Alexandre, M.; Degee, P.; Dubois, P. J Mater Sci 2007, 42, 5105.
17. Solarski, S.; Ferreira, M.; Devaux, E. J Text Inst 2007, 98, 227.
18. Babrauskas, V. NBS-IR 82-2611, U.S. Nat. Bur. Stand. 1982.
19. Babrauskas, V. Fire Mater 1984, 8, 81.
20. Dennis, H. R.; Hunter, D. L.; Chang, D.; Kim, S.; White, J. L.; Cho, J. W.; Paul, D. R. Polymer 2001, 42, 9513.
21. Tanoue, S.; Utracki, L. A.; Garcia-Rejon, A.; Tatibouët, J.; Cole, K. C.; Kamal, M. R. Polym Eng Sci 2004, 44, 1046.
22. Gilman, J. W. Appl Clay Sci 1999, 15, 31.